Biol Trace Elem Res (2008) 122:238–255
DOI 10.1007/s12011-007-8079-2

Prenatal Zinc Deficiency: Influence on Heart Morphology and Distribution of Key Heart Proteins in a Rat Model

Veronica Lopez · Carl L. Keen · Louise Lanoue

Received: 13 September 2007 / Revised: 25 October 2007 / Accepted: 23 November 2007 /
Published online: 26 January 2008

Abstract The etiology of congenital heart disease is multifactorial, with genetics and nutritional deficiencies recognized as causative agents. Maternal zinc (Zn) deficiency is associated with an increased risk for fetal heart malformations; however, the contributing mechanisms have yet to be identified. In this study, we fed pregnant rats a Zn-adequate diet (ZnA), a Zn-deficient (ZnD), or a restricted amount of Zn adequate diet (RF) beginning on gestation day (GD) 4.5, to examine whether increased cell death and changes in cardiac neural crest cells (NCC) play a role in Zn deficiency-induced heart defects. Fetuses were collected on GD 13.5, 15.5, and 18.5 and processed for GATA-4, FOG-2, connexin-43 (Cx43), HNK-1, smooth muscle α-actin (SMA) and cleaved caspase-3 protein expression. Fetuses from ZnA-fed dams showed normal heart development, whereas fetuses from dams fed with the ZnD diet exhibited a variety of heart anomalies, particularly in the region of the outflow tract. HNK-1 expression was lower than normal in the hearts of GD13.5 and 15.5 ZnD fetuses, particularly in the right atrium and in the distal tip of the interventricular septum. Conversely, Cx43 immunoreactivity was increased throughout the heart in fetuses from ZnD dams compared to fetuses from control dams. The distribution and intensity of expression of SMA, GATA-4, FOG-2, and markers of apoptosis were similar among the three groups. We propose that Zn deficiency induced alterations in the distribution of Cx43 and HNK-1 in fetal hearts contribute to the occurrence of the developmental heart anomalies.

Keywords Zinc · Nutrition · Heart development · Cell death · Cardiac neural crest cells · Connexin 43 · HNK-1 · Rat

V. Lopez · C. L. Keen · L. Lanoue (✉)
Department of Nutrition, University of California, Davis, One Shields Ave., Meyer Hall, Davis, CA 95616, USA
e-mail: llanoue@ucdavis.edu

C. L. Keen
Internal Medicine, University of California, Davis, Davis, CA 95616, USA

Introduction

The Food and Drug Organization estimates the prevalence of inadequate Zn intake to be as high as 40% worldwide [1]. Zinc deficiency is particularly common when requirements are increased during periods of rapid growth, such as during infancy, early childhood, and pregnancy [2, 3]. In the USA, the average Zn intake by pregnant women is often below the RDA, and only 60% of women are deemed to have adequate intakes of Zn [4]. Additionally, disease states and environmental insults can induce secondary Zn deficiencies as evidenced by low maternal and fetal Zn concentrations [5]. Collectively, the data support the concept that suboptimal Zn status is common.

Zinc is essential for normal reproduction and development [5, 6], and a severe deficit of Zn can affect the development of multiple organs, including the brain, lungs, skeleton, and heart [7, 8]. Heart development can be particularly sensitive to Zn deficiency. In rats, severe maternal Zn deficiency has been associated with a high incidence of fetal heart anomalies, which were speculated to result in part from a reduced expression of heart-specific genes that contain Zn-finger transcription factor binding sites in their promoter sequence [9]. Although the pathophysiological mechanisms that underlie the heart defects noted above have yet to be delineated, it is recognized that the effects of Zn deficiency are multifaceted. For example, a reduction in cellular Zn can interfere with cellular structure and function [10], influence cell signaling [11, 12], gene transcription [13], and trigger excessive amounts of apoptosis [14–17]. Whereas apoptosis is an integral component of embryonic development, a disruption of apoptotic timing or pattern can result in dysmorphogenesis [18], and a number of teratogens induce congenital malformations as a result of increased cell death [19–21, 22]. With respect to Zn, we and others have reported excessive embryonic cell death after maternal dietary Zn deficiency [15, 23, 24], specifically in regions and tissues that are populated by neural crest cells (NCC), including the somites, visceral arches, optic placodes, limb buds, and the dorsal aspect of the neural tube [25–27].

NCC are essential to support normal heart morphogenesis [28–31] and alterations in the population, the developmental migration, or metabolism of NCC by surgical ablation, genetic deletion, or teratogenic insults lead to a panoply of cardiovascular defects [32–38]. Cardiac NCC originate from the lateral ridges of the neuroectoderm that span between the mid-otic placode and the caudal end of the third somite and contribute ectomesenchymal cells towards the development of the pharyngeal arches, the carotid, subclavian, innominate and coronary arteries, the aorticopulmonary septum, the conotruncal cushions, the distal portion of the ventricular septum, the walls of the ascending aorta, and the pulmonary trunk [28, 29, 39] and participate in the maturation of the cardiac conduction system [29, 38, 40, 41].

Given that the majority of heart anomalies observed in Zn-deficient rat fetuses seem to involve the development of the innominate artery, the great vessels, and the outflow tract [9], we speculated that the heart defects observed with developmental Zn deficiency are due in part to an insult on the population and distribution of NCC as a result of increased cell death. To test this hypothesis, we assessed heart histology at different time points to determine if the abnormal morphology observed in response to Zn deficiency correlated with changes in the distribution of apoptotic cells in fetal rat hearts. To establish the cellular basis of these heart defects, we measured the expression of Connexin (Cx) 43, Smooth Muscle cell Actin (SMA), HNK-1, GATA-4, and Fog-2 using immunocytochemistry. Cx43 is a transmembrane gap junction protein abundantly expressed in cardiac NCC and the embryonic heart [42, 43]. Cx43 is required for the normal development of the outflow tract [44–47], and transgenic mice with targeted loss of function of the Cx43 gene die shortly after birth due to conotruncal heart malformations [48, 49]. In our work, we assessed Cx43

expression as an indicator of cardiac NCC populating the heart, whereas SMA staining was used to trace the abundance of NCC-derived smooth muscle cells [50–52]. We also determined the changes in HNK-1 staining distribution and intensity, as this sulfated carbohydrate epitope is also expressed by NCC; however, in the rats, HNK-1 has also been used as a probe for the components of the cardiac conduction system (CCS) as well [53–61]. Finally, because they potentially may be influenced by Zn status, we monitored the expression of GATA-4 and FOG-2, two Zn-finger transcription factors that regulate the expression of a variety of structural and regulatory genes, critical for cardiac morphogenesis [62–64], but are not associated with cardiac NCC patterning and function. Our results show that Zn deficiency-induced heart anomalies in the developing rat fetuses result partly due to an abnormal distribution of Cx-43 and HNK-1 expressing cells.

Materials and Methods

Animals and Diets Virgin female Sprague–Dawley rats (160–180 g, Charles River Hollister, CA) were fed a purified egg white diet containing adequate Zn (25 μg Zn/g, ZnA) and acclimated for 5 days to their housing conditions. Dams were bred overnight, and the presence of sperm plugs the next morning was noted as gestation day (GD) 0.5. Dams were fed the ZnA diet ad libitum from GD 0.5 to GD 4.5. At GD 4.5, dams were randomly divided into three groups: (1) Zn adequate, ZnA; (2) Zn deficient (<1.0 μg Zn/g, ZnD); or (3) Zn restricted (RF). Dams in ZnA and ZnD groups were allowed unrestricted access to food, whereas dams in the RF group were fed the ZnA diet in amounts equal to those consumed by dams in the ZnD group. The concentration of Zn in the diets was verified using inductively coupled plasma spectrophotometry (ICP, Trace Scan, Thermo-Jarrell Ash, Franklin, MA) after wet ashing with nitric acid as previously described [65]. Maternal food intake and body weight were recorded daily.

Tissue and Plasma Collection Dams were anesthetized by CO_2 inhalation and killed on GD 13.5, 15.5, or 18.5 by heart exsanguination. The liver was excised and plasma was recovered by centrifugation. To determine maternal Zn status, plasma and liver samples were analyzed for Zn concentrations [65].

Cell Death The abundance of apoptotic cells in transverse sections of the heart was determined using terminal deoxynucleotidyl transferase-mediated dUTP nick end labeling (TUNEL) technique (Trevigen, Gaithersburg, MD).

Histology and Immunohistochemistry Fetuses were dissected from their membranes, examined for gross dysmorphology and fixed overnight in 4% paraformaldehyde with continuous rocking at 4°C. Fetuses were dehydrated in a graded series of alcohol washes, cleared in toluene, embedded in paraffin, cut in serial transverse sections (7 μm) using a microtome (American Optical, Buffalo, NY), and collected on slides. A subset of the slides was stained with hematoxylin and eosin and examined for heart morphology under a light microscope. For immunology, slides were incubated in 0.6% H_2O_2 to block endogenous peroxidase activity and permeabilized with trypsin. Non-specific staining was reduced by avidin-biotin (Vector Laboratories, Burlingame, CA) and 10% serum solution incubations. The sections were incubated overnight at 4°C with the following primary antibodies: GATA-4, FOG-2, connexin-43 (Cx43; Santa Cruz Biotechnology, Santa Cruz, CA); HNK-1 and smooth muscle α-actin (SMA; Sigma, St. Louis, MO); caspase-3 and cleaved caspase 3

(Cell Signaling, Beverly, MA), or with a negative control. The next day, the sections were incubated at room temperature with the appropriate biotinylated secondary antibodies, and the antigen-antibody complex was visualized with an avidin-horseradish peroxidase staining kit (ABC, Vector Laboratories), in the presence of 3-3′diaminobenzidine and H_2O_2. Sections were counterstained toluidine blue and examined by light microscopy using a phase microscope (Olympus BX51). Pertinent images were captured using a Qcolor3 digital color camera (Qimaging, BC, Canada). To quantitatively assess expression, staining intensity of each antibody was ranked using a scale of arbitrary units (AU) by two investigators blinded to the treatments. Slides were scored using a 7-point scale where 0.5= light staining and 3=dark staining.

Statistical Analysis All statistical analyses were performed using SAS version 9.0 (SAS Institute, Cary, NC). Significant effects of maternal Zn dietary treatments on reproductive outcomes, maternal plasma and liver Zn concentrations, and heart protein expression were determined by analyses of variance (ANOVA) and least square mean tests. Differences in the incidence of anomalies between groups were tested for statistical significance with chi-square tests. Data are expressed as mean±standard error of the mean (SEM); statistical significance was set at $P<0.05$.

Results

Maternal Outcome Dietary Zn deficiency was initiated on GD 4.5 to minimize pre-implantation losses and continued until dams were killed on GD 13.5, 15.5, or 18.5. Between GD 4.5 and 13.5, food intakes were similar in the ZnA and ZnD groups. Differences in maternal food intake and weight gain began to emerge after GD 13.5, with dams in the ZnD group consuming less food on a daily average than dams in the control group (Table 1). Dams fed with the ZnD diet displayed a 3-day food cycling pattern that is often observed in Zn-deficient rat (Fig. 1). The pair-fed (RF) group was used for the GD 15.5 and GD 18.5 cohorts. The lower food intake that was observed in the ZnD group was reflected by lower maternal weight gains in the ZnD and RF groups compared to controls (Table 1). Maternal plasma Zn concentrations were significantly lower in the ZnD dams than in the ZnA and RF dams (Table 1); maternal liver Zn concentrations were similar among the group (data not shown).

Reproductive Parameters and Incidence of Fetal Anomalies The number of resorptions and malformed fetuses was higher in litters of ZnD dams than in litters from ZnA and RF dams; the number of implantations was similar in the three groups (Table 2). Whereas there was no grossly malformed fetuses in the ZnA and RF groups, approximately half of the litters from dams fed with the ZnD diet had at least one malformed fetus, and the longer the duration of the Zn deficiency, the greater the number of abnormal fetuses within each litter (Table 2). The types and the severity of the anomalies varied with the duration of the gestational Zn deficiency. GD 13.5 fetuses exhibited a preponderance of brain (open forebrain and hindbrain) and facial (microphthalmia, coloboma, and cleft palate) defects, whereas limb (fused/missing digits, deformed or duplicated limbs) and tail anomalies (curly/short tails) were present in greater numbers in GD 15.5 and 18.5 fetuses (Table 3).

Heart Morphology To specifically examine heart morphology, several series of serial transverse sections through the heart (rostral to caudal) were generated from a subset of GD

Table 1 Maternal Food Intake, Body Weight Gain, and Plasma Zn Concentrations

	ZnA	ZnD	RF
GD 4.5 to GD 13.5			
Food Intake (g/day)	20.8±0.8[a]	19.6±0.5	–
Weight Gain (g)	45.4±3.9^{B}	16.1±7.3^{A}	
Plasma Zn (μM)	18.90±0.42^{B}	3.64±047^{A}	–
GD 4.5 to GD 15.5			
Food Intake	21.5±0.4^{B}	15.6±1.1^{A}	14.6±0.9^{A}
Weight Gain	49.3±4.6^{B}	15.3±4.9^{A}	18.5±7.4^{A}
Plasma Zn (uM)	19.83±0.62^{B}	5.39±058^{A}	19.18±1.99^{B}
GD 4.5 to GD 18.5			
Food Intake	22.6±1.4^{B}	14.3±0.6^{A}	14.2±0.8^{A}
Weight Gain	86.3±3.8^{B}	13.0±3.7^{A}	31.5±4.4^{AB}
Plasma Zn (uM)	15.65±1.07^{B}	5.34±1.45^{A}	15.03±0.43^{B}

Different letters indicate significant differences between groups ($P<0.05$) for each period.
[a] Values are means±SEM.

13.5, 15.5, and 18.5 fetuses. All fetuses from dams fed with the Zn-adequate diet (ad libitum and restricted-fed) showed normal heart morphology. In contrast, abnormal heart development was observed in the majority of the fetuses from the ZnD dams. With respect to the type of heart defects, a large proportion of the fetuses of ZnD dams exhibited severe anomalies in the aortic sac, the outflow tract, and the great vessels, suggesting that NCC-derived structures were particularly susceptible to Zn restriction; irregularities in ventricular trabeculation and atrio-ventricular valves formation were also noted. A high frequency of hearts from ZnD fetuses displayed double outlet right ventricle (DORV), with the two large arteries (aorta and pulmonary artery) of the outflow tract stemming from the right ventricle

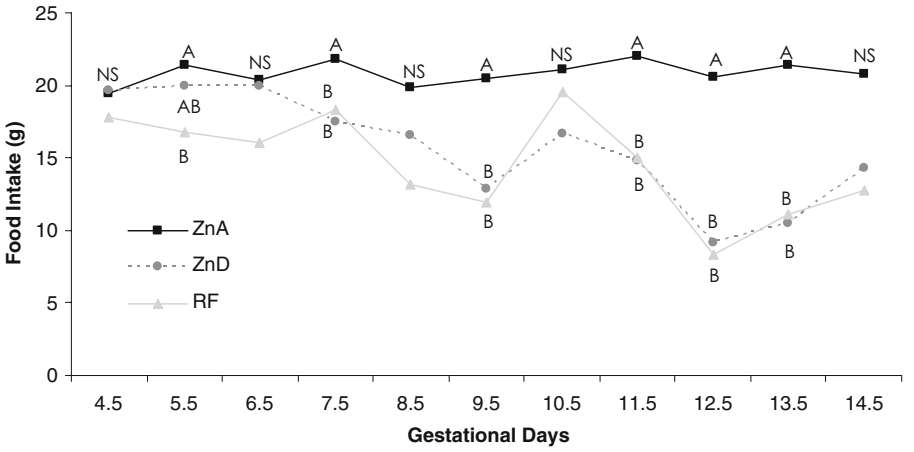

Fig. 1 Maternal daily food intake from GD 4.5 to GD 15.5. Dams were fed ad libitum ZnA (*squares*), or ZnD (*circles*), diets, or a control Zn diet in restricted amounts (RF; *triangles*) Compared to dams fed the ZnA diet, dams fed the ZnD and RF ate significantly less food. Beginning around GD 9.5, dams fed the ZnD diet displayed the typical food cycling pattern associated with Zn deficiency. Results are means±SEM and are the average of six to nine dams per group. Different superscripts indicate significant differences ($P<0.05$)

Table 2 Reproductive Outcome Data

Gestation Day	Diet	No. of Litters	No. of Implantations[a]	No. of Resorptions per Litter[a]	No. of Litters with > 1 Resorption (%)	No. of Malformed Embryos per Litter[a]	No. of Litters with > 1 Malformed Embryo (%)
13.5[b]	ZnA	10	14.0±0.49	0.50±0.22	4 (40)	0	0
	ZnD	14	13.7±0.59	1.36±0.67	6 (43)	1.29±0.63	5 (36)
15.5[c]	ZnA	11	13.2±0.76	0.18 ± 0.12^{A}	2 (18)	0^{a}	0
	ZnD	15	14.0±0.39	1.87 ± 0.60^{B}	9 (60)	2.67 ± 0.78^{B}	10 (67)
	RF	5	12.6±0.87	0^{A}	0	0^{A}	0
18.5[d]	ZnA	8	13.3±0.53	0.25 ± 0.16^{A}	2 (25)	0^{A}	0
	ZnD	13	13.2±0.55	1.38 ± 0.71^{B}	6 (46)	3.07 ± 1.08^{B}	7 (54)
	RF	7	11.8±0.40	0.57 ± 0.37^{A}	2 (29)	0^{A}	0

Different letters indicate significant differences between groups ($P<0.05$).

[a] Results are means±SEM.

[b] Results from GD13.5 ANOVA: number of implantations, NS; number of resorptions, NS; number of malformed embryos, NS

[c] Results from GD 15.5 ANOVA: number of implantations, NS; number of resorptions, $P<0.02$; number of malformed embryos, $P<0.007$

[d] Results from GD 18.5 ANOVA: number of implantations, NS; Number of resorptions, $P<0.02$; number of malformed embryos $P<0.02$

instead of their respective ventricular outlets. Anomalies of the ventricular septum were present in a number of ZnD hearts often associated with overriding and misplacement of the heart valves.

By GD 13.5, the heart has typically matured into a septated four-chambered organ. In the Zn-adequate group, the outflow tract connecting the ventricles to the aortic sac had undergone extensive remodeling with the formation of the aorticopulmonary septum coincident with the infiltration of the cardiac NCC into the endotruncal cushions. Zinc

Table 3 Effects of Maternal Dietary Zinc on the Incidence of Fetal Anomalies

Gestation Day	Diet	No. of Live Embryos (%)	No. of Malformed Embryos (%)	Total Number of Fetuses with Specific Anomalies (%)					
				Brain[a]	Facial[a]	Heart[a]	Limb[a]	Tail[a]	Others
13.5	ZnA	135 (96.3)	0	0	0	0	0	0	0
	ZnD	173 (90.6)	18 (9.7)	15 (7.7)	2 (1.0)	4 (2.0)	1 (0.5)	7 (4.0)	0
15.5[b]	ZnA	144 (98.9)	0^{A}	0	0	0	0^{A}	0^{A}	0
	ZnD	182 (86.4)	$40\ (25.3)^{B}$	6 (3.9)	7 (2.3)	8 (5.9)	$24\ (14.3)^{B}$	$19\ (12.6)^{B}$	6(4.4)
	RF	63 (100)	0^{A}	0	0	0	0^{A}	0^{A}	0
18.5[c]	ZnA	105 (98.1)	0^{A}	0	0	0	0	0^{A}	0
	ZnD	153 (88.3)	$40\ (30.2)^{B}$	6 (3.9)	4 (2.2)	1 (0.5)	9 (4.4)	$27\ (20.7)^{B}$	5 (16.7)
	RF	79 (95.4)	0^{A}	0	0	0	0	0^{A}	0

[a] Brain anomalies include swollen hindbrain and shortened forebrain; facial anomalies include small or no eyes and cleft palate; limb anomalies include fused and missing digits; and tail anomalies include curly, short or absent tail; others include gastroschisis, kinked spine, and blood pooling.

[b] Results from GD 15.5 ANOVA: malformed embryos, $P<0.007$; limb, $P<0.02$; tail, $P<0.04$

[c] Resutls from GD 18.5 ANOVA: malformed embryos, $P<0.02$; tail, $P<0.01$

deficiency affected the morphogenesis of the outflow tract, such that the aortico-pulmonary septum appeared to lack the proper curvature and was misaligned vis-à-vis the left ventricle (data not shown). Despite the above, fetuses from the ZnD dams did not show overt septation defects. At GD 15.5, the arteries (sub-clavian and carotid) derived from the aortic arch were clearly visible in fetal hearts of ZnA dams (Fig. 2a). In contrast, a number of these arteries were small or missing in ZnD hearts, perhaps a result of abnormal septation or alignment of the outflow tract as shown in Fig. 2d. Additionally, in the fetuses' hearts of ZnA dams, the outflow tract was completely septated into the two outflow arteries of the left and right ventricles, the aorta and the pulmonary trunk (Fig. 2b), whereas we observed irregular septation of the outflow tract in fetuses from the ZnD dams, particularly in the

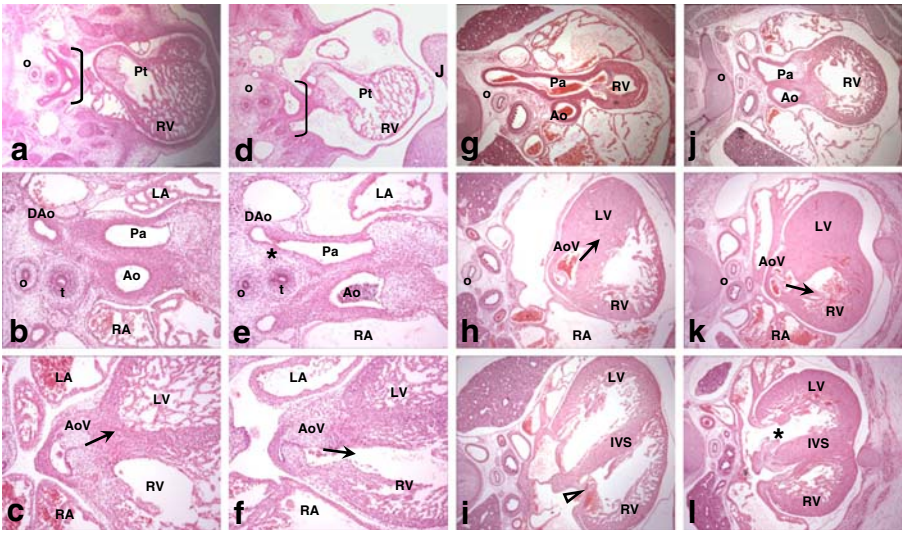

Fig. 2 Photomicrographs of transverse sections of GD 15.5 (**a**–**f**) and GD 18.5 (**g**–**l**) hearts of fetuses from dams fed a ZnA (**a**–**c** and **g**–**i**) or a ZnD (**d**–**f** and **j**–**l**) diets (images from the RF group are not shown as heart morphology was similar to that of controls) and stained with hematoxylin and eosin. GD**15.5** hearts: **a** *Bracket* showing aortic arch arteries originating from aorta in fetuses from ZnA dams. **d** Bracket showing incomplete/missing aortic arch arteries and abnormal distal outflow tract in ZnD fetuses; heart and pulmonary trunk are distorted; pericardium is swollen. **b** Rostral sections of hearts from fetuses of ZnA dams showing the proximal portion of the ascending aorta (*Ao*), the pulmonary trunk (*PT*) and the descending aorta (*DAo*). **e** Similar heart structures in fetuses of ZnD dams; note the distended aspect of both aortic and pulmonary artery trunks with thin endothelium and the overall mis-alignment of the OFT; incomplete separation of the DAo. **c** Normal aortic valves (*AoV*) and leaflets originating from the left ventricle (*LV*, *arrows*), in ZnC hearts. **f** Abnormal aortic leaflets and abnormal position of the aortic valves entering the right ventricle (*RV*, *arrow*) instead of the left (*LV*) in ZnD hearts. *GD 18.5 hearts*: **g** Complete septation of the ouflow tract into aorta and pulmonary artery in ZnA hearts. **j** DORV in ZnD hearts: abnormal septation of the outflow tract resulting in both the aorta and pulmonary artery trunks in right ventricle. **h** Aortic valve (*AoV*) inlets originating from the distal portion of the left ventricle (*LV*, *arrows*) in fetuses of ZnA dams. **k** Abnormal positioning of the aorta with the valves stemming from the right ventricle outlet (*RV*) instead of the left (*arrow*) in fetuses of ZnD dams. **i** Caudal heart sections of fetuses from ZnA dams showing the leaflets of the right (tricuspid, *tri*) and left (mitral, *mi*) atrio-ventricular valves (*arrow heads* and *asterisks*) and the interventricular septum (IVS). **l** Irregular formation and placement (overriding) of the tricuspid valve (*arrow head*) and incomplete and/or absent mitral valve (*asterisk*) in ZnD hearts; thickening of the interventricular septum leading to a narrow right ventricle (*RV*) lumen. Photomicrographs are ×4 (A, D, G, J) and ×10. Legend: *o* esophagus; *t* trachea; *RA/LA* right and left atrium; *RV/LV* right and left ventricle; *Pt* pulmonary trunk; *Pa* pulmonary artery; *Ao* aorta; *Dao* dorsal aorta; *AoV* aortic valve; *IVS* invertricular septum; *PC* pericardium; *DORV* double outlet right ventricle

proximal region (Fig. 2e). Zn deficiency was also associated with irregularly shaped ascending and descending aorta and distended pulmonary tract (Fig. 2e). In caudal sections, fetuses from dams in the ZnD group had anomalies in aortic valve formation and positioning (compare Fig. 2c,f) and thickening of the endotruncal cushions resulting in complete stenosis of the pulmonary trunk and/or a reduction of the aortic lumen (data not shown). Similar to the irregularities in the positioning of aortic valves observed in GD 15.5 ZnD fetuses, the hearts of GD 18.5 ZnD fetuses exhibited alignment anomalies such as DORV (Fig. 2j), dextraposed aortas, resulting in the aorta and aortic valves inlets stemming from the right ventricle instead of the left (Fig. 2k). Aberrations in the tricuspid valves were observed in some fetuses from the ZnD dams (Fig. 2l), and in some cases, this was associated with an unequal atrio-ventricular connection and/or a reduced right ventricle chamber (Fig. 2l).

Persistent truncus arteriosus, a characteristic phenotype observed after NCC ablation in chick embryos, was observed in only one fetus from the ZnD dams; all of the remaining OFT examined were septated. However, Zn deficiency was associated with irregular patterning of septation, often resulting in misalignment of the septum positioning vis-à-vis the ventricles, with a rightward displacement of the aortic trunk (DORV). Several of the fetuses from ZnD dams had one or more of the arch arteries missing or irregularly shaped whereas in one Zn-deficient fetus, the ductus arteriosus passed to the right of the trachea instead of the left.

Cell Death and Cleaved Caspase-3 One consequence of developmental Zn deficiency can be excessive and inappropriate apoptosis [14]. Whereas apoptotic cells were present in specific regions of the heart, particularly in the outflow tract septum (GD 13.5) and the endocardial cushions (GD 15.5), the amount of overall cell death assessed by TUNEL was minimal in all groups. Fetuses from ZnD dams tend to display a higher number of TUNEL-positive cells in the proximal region of the outflow tract (Fig. 3b) compared to fetuses from ZnA dams (Fig. 3a), but these differences were not significant. As Zn deficiency has been associated with increased apoptosis via caspase-3 activation, we probed the fetal hearts with a cleaved caspase-3 antibody, a hallmark of programmed cell death. Similar to above, GD 13.5 and 15.5 fetuses had a limited number of cleaved caspase-3 expressing cells in regions of the outflow tract and cushions with no differences among Zn treatment groups (Fig. 3c,d; Table 4). Cell death was not detected in GD 18.5 fetuses with either marker (data not shown).

SMA and Cx43 Expression Overall, the heart had an abundant expression of SMA with no differences in the distribution and intensity of immunoreactive signal among the two groups at a given gestation day (Fig. 4a–d). GD 13.5 fetuses from ZnD dams had significantly high Cx43 immunoreactivity throughout the heart including the outflow tract, which does not normally express Cx43 (Fig. 5d,e), in contrast to fetuses of ZnA dams, which showed light Cx43 staining, and limited to the myocardium (Fig. 5a,b). Similarly, when heart sections of GD 15.5 fetuses were examined, those of the ZnD group showed strong and widespread Cx43 expression, extending to the pulmonary, aortic, mitral, and tricuspid valves and the proximal portion of the conotruncal cushion (Fig. 5f), compared to the ZnA fetuses, where Cx43 was detected only in the trabeculae and the pericardium and not in the cushion (Fig. 5c). At GD 18.5, Cx43 staining was similar in all groups (data not shown).

HNK-1 Expression The antibody HNK-1 (human natural killer cell-1) was used as a marker of NCC. HNK-1 positive cells were observed in a limited number of specific structures including the heart. In GD 13.5 fetuses, HNK-1 positive cells were detected in the basal

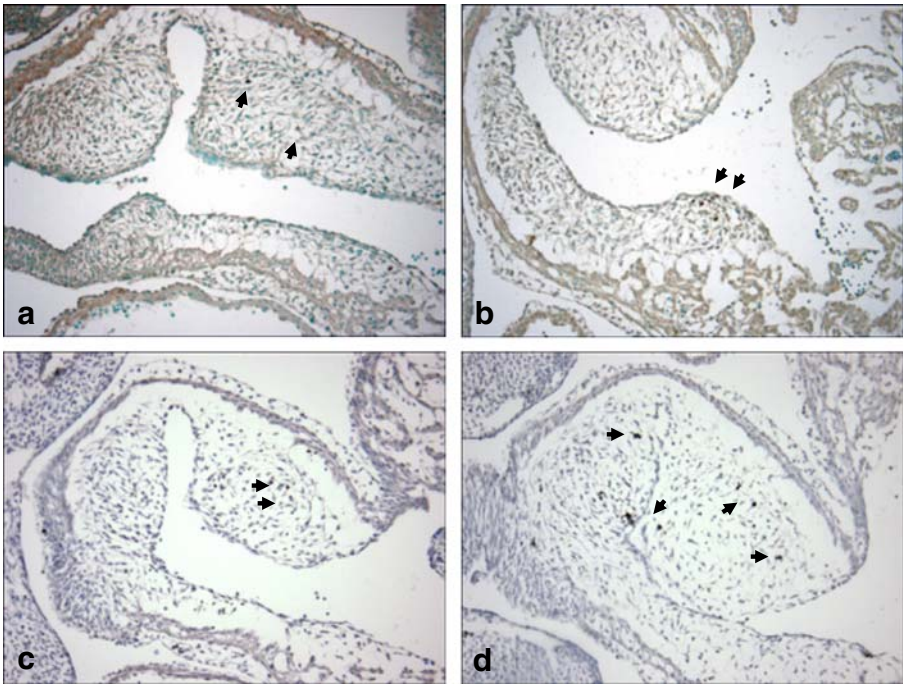

Fig. 3 Effects of maternal Zn deficiency on TUNEL (**a**, **b**) and cleaved caspase-3 (**c**, **d**) expression in GD 13.5 fetal outflow tracts. A limited number of apoptotic cells were detected in the aortico-pulmonary spiral septum of GD 13.5 fetuses using the TUNEL assay or caspase 3 immunoreactivity (*arrow heads*), and results among fetuses of ZnA (**a**, **c**) were similar to those observed in fetuses of ZnD (**b**, **d**) groups. Photomicrographs are ×20 magnification

Table 4 Effects of Maternal Zn Deficiency on the Expression of HNK-1, Cx43, and Cell Death Markers

	GD 13.5		GD 15.5	
	ZnA (6–10)[a]	ZnD (4–8)	ZnA (3–4)	ZnD (6–9)
HNK-1[c]	2.33±0.21[b]	1.83±0.24	1.69±0.34	0.83±0.30
Cx43[d]	1.38±0.83	3.81±0.92	2.83±0.17	5.43±1.55
Caspase3[e]	6.42±0.99	5.56±1.32	3.69±1.77	2.50±0.89
TUNEL[f]	2.15±0.48	1.85±0.56	4.17±1.21	2.44±0.79

[a] Number in parentheses indicate number of hearts examined for protein expression.

[b] Values are mean±SEM. Staining was scored by qualitative assessment by two observers blinded to experimental treatments using a 7-point scale (0–3) where 0.5=light staining and 3=dark staining.

[c] HNK-1: *GD13.5 hearts* total score of IVS (interventricular septum) + RA (right atrium); *GD15.5 hearts* total score of IVS + EC (endocardial cushions)

[d] Cx43: *GD13.5 hearts* total score of IVS + EC + OFT (outflow tract); *GD15.5 hearts* total score of OFT + PT (pulmonary trunk) + Av (atrial valve) + Pv (pulmonary valve) + M (mitral valve) + T (tricuspid valve)

[e] Caspase3: *GD13.5 hearts* total score of OFT + IVS + LV (left ventricle) + RV (right ventricle) + EC; *D15.5 hearts* total score of OFT + Av + IVS +

[f] TUNEL: *GD13.5 hearts* total score of OFT + RV + LV + EC + IVS; *GD15.5 hearts* total score of PT + IVS + EC

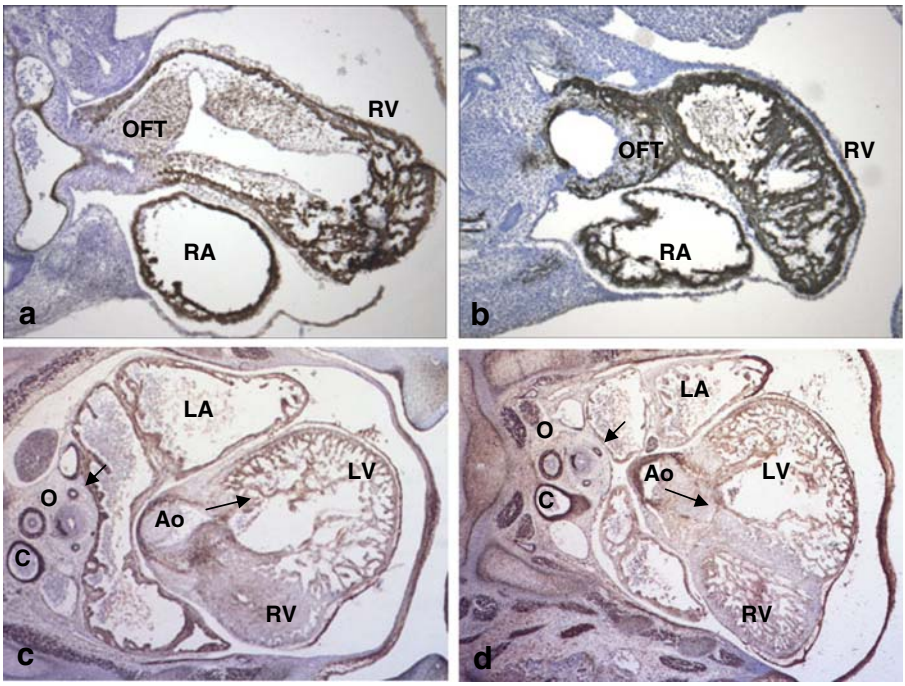

Fig. 4 Photomicrographs of transverse sections GD 13.5 (**a**, **b**; ×10) and GD 15.5 (**c**, **d**; ×4) fetal hearts from ZnA (**a**, **c**) and ZnD (**b**, **d**) showing smooth muscle cells actin (*SMA*) immunopositive cells. On both days of gestation, hearts of ZnA (**a**, **c**) and ZnD (**b**, **d**) fetuses show similar pattern and intensity of staining, despite morphological differences between the two groups: note the *arrows* showing the small and misaligned arteries and pointing to the aortic trunk (*Ao*) originating from the right ventricle (*RV*) instead of the left (*LV*) in GD 15 ZnD hearts. *C* Subclavian artery; *O* esophagus; *LA*, *RA* left and right atrium; *LV*, *RV* left and right ventricle; *OFT* outflow tract

plate (marginal layer) of the neural tube and in the heart. In the hearts of fetuses from ZnA dams, strong HNK-1 immunoreactivity was observed in the distal tip of the interventricular septum (IVS), where the bundle of His is located, the posterior part of the right atrioventricular node (AVN), and discrete cells within the right and left ventricle myocardium (Fig. 6a,b). In contrast, the intensity and dispersion of HNK-1 expression was reduced in fetuses from ZnD dams, particularly in the heart, where it was limited to the distal tip of the IVS with no staining in the right atrium (Fig. 6c,d); these differences did not reach statistical significance (Table 4). At GD 15.5, HNK-1 staining was present in the spinal cord (mantle and marginal layers), thoracic vertebra, dorsal root and sympathic ganglia, carotid artery, cardinal veins, and endocardial cushions of the interventricular septum of the heart (Fig. 6e,g). We observed similar HNK-1 expression patterns among groups in all tissues (e.g., spinal cord and ganglia) but the hearts, where ZnD fetuses had minimal staining compared to ZnA and RF fetuses, particularly to the left of the atrio-ventricular cushion, possibly the atrio-ventricular node (Fig. 6h vs f); these differences in staining intensity were statistically significant (Table 4). By GD18.5, HNK-1 staining in the heart has greatly diminished; only a few loci of positive cells were noted in the myocardium of the ventricles and the walls of the pulmonary trunk in fetuses from ZnA dams (Fig. 6k), and HNK-1 staining was absent in fetuses from ZnD dams (Fig. 6l).

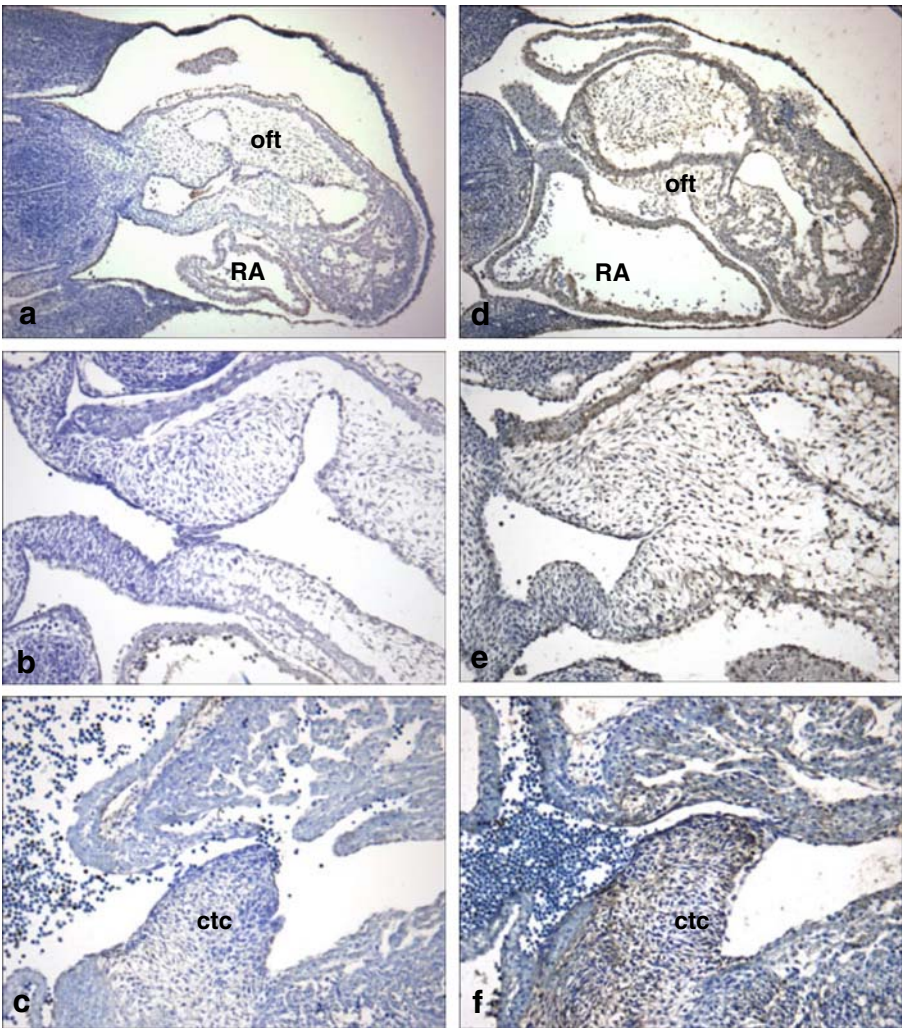

Fig. 5 Photomicrographs of GD 13.5 (**a**, **b** and **d**, **e**) and GD 15.5 (**c**, **f**) hearts from ZnA (**a**–**c**) and ZnD (**d**–**f**) fetuses, stained with Cx-43 antibody. In GD 13.5 ZnA fetuses (**a**, **b**), Cx-43 staining was light and limited to the ventricle myocardium. In contrast, strong Cx43 staining can be observed in the ventricle trabeculae and throughout the outflow tract of ZnD hearts (**b**, **c**). On GD 15.5, Cx43 staining was present in the proximal portion of the conotruncal cushion (*ctc*) of ZnD hearts but not in ZnA fetuses. Photomicrographs are ×10 (**a**, **b**) and ×20 (**c**, **f**). *oft* Outflow tract; *ctc* conotruncal cushion; *RA* right atrium

GATA-4 and FOG-2 Expression The profile of GATA-4 and FOG-2 distribution in GD 15.5 fetal hearts (Fig. 7a–h) resembled closely that of GD 18.5 hearts (Fig. 7i–p); with similar levels of staining intensity between the two dietary Zn treatments (Fig. 7b and f vs d and h). For GATA-4, strong staining was detected in the nuclei of the myocardial cells of the ventricles (Fig. 7a,c) and of the atrio-ventricular cushion (Fig. 7b,d), whereas FOG-2 expression was restricted to the trabeculated ventricles (Fig. 7e,g) with no staining present in the endocardial cushions (Fig. 7f,h). Of note, in contrast to the nuclei localization of GATA-4, FOG-2 was expressed throughout the cells.

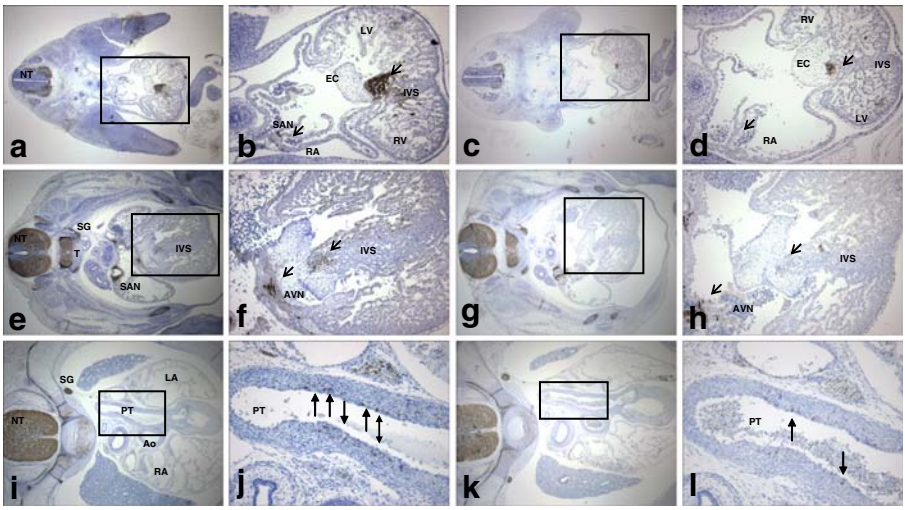

Fig. 6 HNK-1 staining of transverse sections of GD 13.5 (**a**–**d**), GD 15.5 (**e**–**h**), and GD 18.5 (**i**–**l**) fetuses from ZnA (**a**, **b**; **e**, **f**; **i**, **j**) and ZnD (**c**, **d**; **g**, **h**; **k**, **l**) dams. GD 13.5 fetuses from ZnA dams (**a**, **b**) show increased HNK-1 staining in the basal plate of the neural tube (*NT*), the tip of the interventricular septum (*IVS*) and in right atrium (*RA*) region corresponding to the sino-atrial node (*SAN*) compared to GD 13.5 fetuses from ZnD dams (**c**, **d**). In GD 15.5 fetuses of ZnA dams (**e**, **f**), cells stained positive for HNK-1 in the neural tube, the thoracic vertebrae (*T*), the sympathic ganglion (*SG*) and in the SAN. ×10 photomicrographs (**b**, **d**) show heart HNK-1 expression. *Arrows* show increased HNK-1 positive stain cells in the dorsal portion of the endocardial cushion (*EC*) and IVS tip of fetuses from ZnA (**g**) dams compared to fetuses from ZnD dams (**h**). HNK-1 expression in heart sections of GD 18.5 fetuses from ZnA (**i**, **j**) and ZnD (**k**, **l**) dams. At this stage of development, only a limited number of heart cells were positively stained for HNK-1, both in ZnA and ZnD fetuses, including the walls of the pulmonary trunk (*PT*) and the aorta (*Ao*). At higher magnification (×20), ZnA fetuses (**j**), had a greater proportion of HNK-1 positive cells in the walls of the pulmonary trunk (*boxed region*, *arrows*) compared to ZnD (**l**). *NT* Neural tube; *T* thoracic vertebra; *SG* sympathic ganglion; *RA*, *LA* right and left atrium; *RV, LV* right and left ventricle; *IVS* interventricular septum; *Ao* aorta; *PT* pulmonary trunk; *EC* endocardial cushion; *SAN* sino-atrial node; *AVN* atrio-ventricular node

Discussion

Using a rat model, we show herein that maternal dietary Zn is an important determinant of normal heart development. The observation that heart anomalies were present in fetuses from ZnD dams but not in fetuses from RF dams supports the idea that these defects occurred as a consequence of Zn depletion, rather than from the general reduction in food intake that often accompanies Zn deficiency. As congenital heart defects, the most common type of structural birth defects [66, 67], are known to result from genetic and environmental insults interactions, these data are relevant, as they suggest that maternal Zn status can be a modulating factor in determining an unfavorable outcome when a genetic susceptibility is already present.

Similar to those previously reported by our group and others [5, 9, 68], the teratogenic outcomes that we observed in fetuses from dams fed the ZnD diet involved heart structures and vascular segments, where normal development depends on the proper infiltration and differentiation of cardiac NCC, and included, but were not limited to, other tissues populated by NCC such as the face (lip, palate, and eyes) and the thymus. As Zn depletion can lead to caspase 3 activation and increased cell death [14, 17, 69], we investigated the

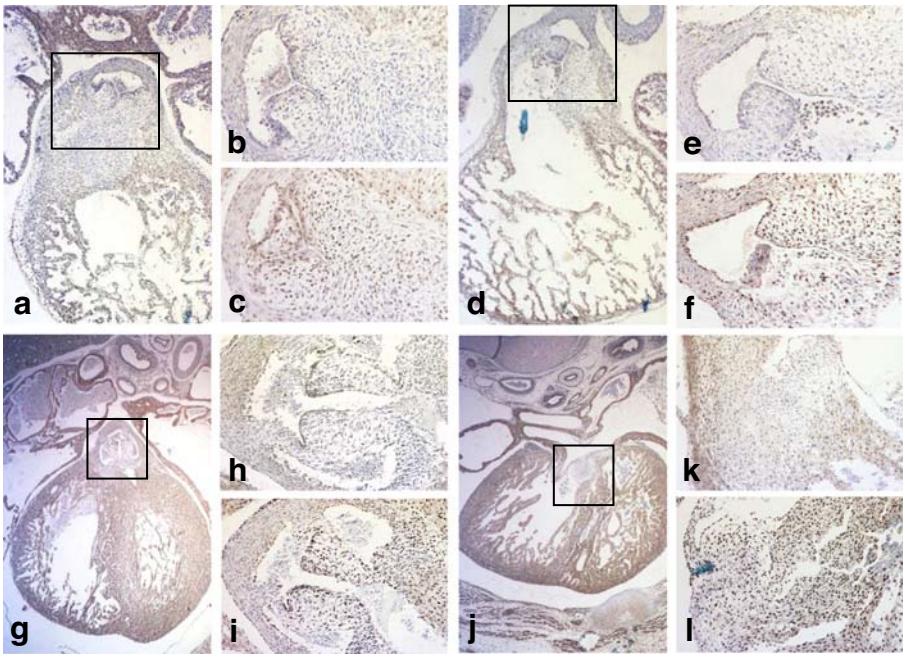

Fig. 7 Transverse sections of GD 15.5 (**a**–**f**), GD 18.5 (**g**–**l**) fetal hearts from ZnA (**a**–**c** and **g**–**i**) and ZnD (**d**–**f** and **j**–**l**) dams. At either time points, FOG-2 and GATA-4 expression were similar between ZnA and ZnD hearts. Note the nuclei localization of GATA-4, whereas FOG-2 is expressed throughout the cells (**a**, **d**, **g**, and **j**). Also noteworthy is the apparent restriction of FOG-2 but not GATA-4 in the endocardial valve cushions and leaflets (**b** vs **c**; **e** vs **f**; **h** vs **i**; **k** vs **l**)

idea that developmental Zn deficiency has reduced the population of NCC targeting to the heart. Our results, which show higher number of apoptotic cells in Zn deficient hearts but not in regions populated by NCC, do not support this hypothesis. This was against our expectations as NCC are thought to be particularly sensitive to teratogens, and numerous insults have been shown to trigger excessive cell death in this cell population [19, 21, 70, 71].

Importantly, we need to point out that we cannot rule out the possibility that maternal Zn deficiency has killed the progenitor cardiac NCC, in situ, within the neuroepithelium and that a secondary wave of late migrating NCC may have compensated for the earlier loss of NCC. Boot et al. [72], have suggested that there are two subpopulations of cardiac NCC emerging from the dorsal side of the embryo at different times (early and late migrating), and these late-migrating NCC have been shown to contribute to forming heart structures in the absence of earlier-migrating NCC [73]. However, as the patterns and intensity of SMA staining was not affected by Zn deficiency, it is likely that the survival of cardiac NCC was unaffected in Zn-deficient rat fetuses. Consistent with this idea is the observation that the OFT anomalies in our model show incomplete penetrance and do not recapitulate the full spectrum or the severity of the manifestations resulting from complete deletion of cardiac NCC through genetic and surgical manipulations [29, 74].

It should be noted however that we did observe in the Zn-deficient fetuses some of the anomalies typically associated with a disturbance of cardiac NCC, including a high frequency of DORV, with both the aorta and the pulmonary trunks stemming from the right ventricle, ventricular septal defects (VSD) often accompanied with an overriding tricuspid

valve, and missing or stenotic aortic arch arteries, suggesting more subtle perturbations of NCC, perhaps changes in the migration or distribution of NCC within the heart. An interesting finding in the current study was the transient increased expression and distribution of Cx43 in the fetal heart during Zn deficiency. Cx43 staining intensity was increased in the heart trabeculae, where the protein is normally expressed and expanded to structures not normally expressing Cx43 (OFT and valves). Perhaps, the increased Cx43 in the Zn-deficient heart reflects an attempt to recruit a dwindling population of NCC. Although the molecular and cellular bases for these changes are unclear, one alternate possibility is that Zn deficiency might upregulate Cx43 gene expression. As the promoter region of Cx43 contains multiple consensus sequences for AP1 and Sp1 binding [75, 76], low intracellular Zn level has been associated with increased AP1-DNA binding activity in other cell types [77, 78]. Of note, rat fetuses exposed to the herbicide nitrofen exhibit outflow tract and great vessel defects and show a transient increased expression of Cx43 in the heart [79]. It has also been suggested that the cardiac outflow defects observed after hyperhomocysteinemia can be in part due to elevated Cx43 levels [80]. We suggest that the aberrant pattern of Cx43 expression observed in our model contributes to the teratogenicity of Zn deficiency.

In addition to modulating the abundance of NCC reaching the outflow tract by regulating their migration and deployment [44, 81], Cx43 have been shown to modulate NCC migration by modulating surrounding non-crest cells [45]. Thus, impaired development of myocardial cells could be another pathophysiologic consequence of abnormal Cx43 heart dosage. Mice with a targeted loss of function of the Cx43 gene for example also exhibit conduction defects in addition to conotruncal malformations [48, 49, 82, 83]. Interestingly, in our model of Zn deficiency, we show reduced HNK-1 expression in the heart, in regions that are in close proximity of certain components of the CCS (namely, the SAN and AVN). The interpretation of these results is challenging as HNK-1 has been used to probe both the NCC and the components of the CCS [53–61].

As cre recombinase technology is not available for rats, we have a limited ability at this time to tract the various cell types that contribute to heart development in these fetuses. However, a number of recent studies using transgenic mice with NCC specific cre recombinase activity have shown that NCC not only migrate within the cells of the conduction system lineage but that they play a significant role in their final maturation [38, 40, 41]. Gurjarpadhye et al. [34] have also observed abnormal conductivity in hearts of chick embryos after the ablation of their cardiac NCC. Thus, consistent with the above, we postulate that Zn deficiency could affect either the development of the conduction system directly or the ability of NCC to participate in CCS maturation and innervation; either effect would result in impaired heart formation.

In summary, our data support the concept that severe maternal zinc deficiency can result in a number of cardiac anomalies, particularly in structures whose complete maturation is dependent on NCC. Whereas the changes in HNK-1 and Cx43 could be secondary to the abnormal heart development and not causal, we show that the development of structures that depend on the proper migration of NCC seems particularly vulnerable to these changes. Although the definitive mechanism(s) that make Zn essential to normal fetal heart development remain unclear, we propose that a Zn deficiency-induced alteration in the expression of Cx43 and HNK-1 proteins contributes to abnormal heart development, perhaps via disturbing the normal pattern of NCC migration.

Acknowledgments This work was supported in part by grants from National Institutes of Health: HD-01743, T32-DK07355, and DK35747.

References

1. Maret W, Sanstead HH (2006) Zinc requirements and the risks and benefits of zinc supplementation. J Trace Elements Med Biol 20:3–18
2. Powell SR (2000) The antioxidant properties of zinc. J Nutr 130:1447S–1454S
3. Kelishadi R, Alikhassy H, Amiri M (2002) Zinc and copper status in children with high family risk of premature cardiovascular disease. Ann Saudi Med 22:291–294
4. Briefel RR, Bialostosky K, Kennedy-Stephenson J, McDowell MA, Ervin RB, Wright JD (2000) Zinc intake of the U.S. population: findings from the third National Health and Nutrition Examination Survey. 1988–1994. J Nutr 130:1367S–1373S
5. Keen CL, Hanna LA, Lanoue L, Uriu-Adams JY, Rucker RB, Clegg MS (2003) Developmental consequences of trace mineral deficiencies in rodents: acute and long-term effects. J Nutr 133:1477S–1480S
6. Dufner-Beattie J, Huang ZL, Geiser J, Xu W, Andrews GK (2006) Mouse ZIP1 and ZIP3 genes together are essential for adaptation to dietary zinc deficiency during pregnancy. Genesis 44:239–251
7. Keen CL (1996) Teratogenic effects of essential trace metals: deficiency and excesses. In: Chang LW, Magos L, Suzuki T (eds) Toxicology of metals. CRC, New York, pp 977–1001
8. Rogers JM, Keen CL, Hurley LS (1985) Zinc deficiency in pregnant Long-Evans hooded rats: teratogenicity and tissue trace elements. Teratology 31:89–100
9. Duffy JY, Overmann GJ, Keen CL, Clegg MS, Daston GP (2004) Cardiac abnormalities induced by zinc deficiency are associated with alterations in the expression of genes regulated by the zinc-finger transcription factor GATA-4. Birth Defects Res B Dev Reprod Toxicol 71:102–109
10. Mackenzie GG, Zago MP, Aimo L, Oteiza PI (2007) Zinc deficiency in neuronal biology. IUBMB Life 59:299–307
11. Beyersmann D, Haase H (2001) Functions of zinc in signaling, proliferation and differentiation of mammalian cells. Biometals 14:331–341
12. Merten KE, Jiang Y, Kang YJ (2007) Zinc inhibits doxorubicin-activated calcineurin signal transduction pathway in H9c2 embryonic rat cardiac cells. Exp Biol Med (Maywood) 232:682–689
13. Aimo L, Oteiza PI (2006) Zinc deficiency increases the susceptibility of human neuroblastoma cells to lead-induced activator protein-1 activation. Toxicol Sci 91:184–191
14. Clegg MS, Hanna LA, Niles BJ, Momma TY, Keen CL (2005) Zinc deficiency-induced cell death. IUBMB Life 57:661–669
15. King LE, Osati-Ashtiani F, Fraker PJ (2002) Apoptosis plays a distinct role in the loss of precursor lymphocytes during zinc deficiency in mice. J Nutr 132:974–979
16. Chou SS, Clegg MS, Momma TY, Niles BJ, Duffy JY, Daston GP, Keen CL (2004) Alterations in protein kinase C activity and processing during zinc-deficiency-induced cell death. Biochem J 383:63–71
17. Min YK, Lee JE, Chung KC (2007) Zinc induces cell death in immortalized embryonic hippocampal cells via activation of Akt-GSK-3beta signaling. Exp Cell Res 313:312–321
18. Mirkes PE (2002) 2001 Warkany lecture: to die or not to die, the role of apoptosis in normal and abnormal mammalian development. Teratology 65:228–239
19. Dunty WC, Chen SY, Zucker RM, Dehart DB, Sulik KK (2001) Selective vulnerability of embryonic cell populations to ethanol-induced apoptosis: implications for alcohol-related birth defects and neurodevelopmental disorder. Alcohol Clin Exp Res 25:1523–1535
20. Little SA, Mirkes PE (2002) Teratogen-induced activation of caspase-9 and the mitochondrial apoptotic pathway in early postimplantation mouse embryos<. Toxicol Appl Pharmacol 181:142–151
21. Sulik KK, Cook CS, Webster WS (1988) Teratogens and craniofacial malformations: relationships to cell death. Development 103(Suppl):213–231
22. Thayer JM, Mirkes PE (1995) Programmed cell death and N-acetoxy-2-acetylaminofluorene-induced apoptosis in the rat embryo. Teratology 51:418–429
23. Hanna LA, Clegg MS, Momma TY, Daston GP, Rogers JM, Keen CL (2003) Zinc influences the in vitro development of peri-implantation mouse embryos. Birth Defects Res A Clin Mol Teratol 67:414–420
24. Osati-Ashtiani F, King LE, Fraker PJ (1998) Variance in the resistance of murine early bone marrow B cells to a deficiency in zinc. Immunology 94:94–100
25. Harding AJ, Dreosti IE, Tulsi RS (1988) Zinc deficiency in the 11 day rat embryo: a scanning and transmission electron microscope study. Life Sciences 42:889–896
26. Jankowski-Hennig MA, Clegg MS, Daston GP, Rogers JM, Keen CL (2000) Zinc-deficient rat embryos have increased caspase 3-like activity and apoptosis. Biochem Biophys Res Commun 271:250–256
27. Rogers JM, Taubeneck MW, Daston GP, Sulik KK, Zucker RM, Elstein KH, Jankowski MA, Keen CK (1995) Zinc deficiency causes apoptosis but not cell cycle alterations in organogenesis-stage rat embryos: effect of varying duration of deficiency. Teratology 52:149–159

28. Hutson MR, Kirby ML (2003) Neural crest and cardiovascular development: a 20-year perspective. Birth Defects Res C Embryo Today 69:2–13
29. Hutson MR, Kirby ML (2007) Model systems for the study of heart development and disease Cardiac neural crest and conotruncal malformations. Semin Cell Dev Biol 18:101–110
30. Waldo K, Miyagawa-Tomita S, Kumiski D, Kirby ML (1998) Cardiac neural crest cells provide new insight into septation of the cardiac outflow tract: aortic sac to ventricular septal closure. Dev Biol 196:129–144
31. Waldo KL, Hutson MR, Stadt HA, Zdanowicz M, Zdanowicz J, Kirby ML (2005) Cardiac neural crest is necessary for normal addition of the myocardium to the arterial pole from the secondary heart field. Dev Biol 281:66–77
32. Epstein JA, Li J, Lang D, Chen F, Brown CB, Jin F, Lu MM, Thomas M, Liu E, Wessels A, Lo CW (2000) Migration of cardiac neural crest cells in Splotch embryos. Development 127:1869–1878
33. Fujino H, Nakagawa M, Nishijima S, Okamoto N, Hanato T, Watanabe N, Shirai T, Kamiya H, Takeuchi Y (2005) Morphological differences in cardiovascular anomalies induced by bis-diamine between Sprague–Dawley and Wistar rats. Congenit Anom (Kyoto) 45:52–58
34. Gurjarpadhye A, Hewett KW, Justus C, Wen X, Stadt H, Kirby ML, Sedmera D, Gourdie RG (2007) Cardiac neural crest ablation inhibits compaction and electrical function of conduction system bundles. Am J Physiol Heart Circ Physiol 292:H1291–1300
35. Kaartinen V, Dudas M, Nagy A, Sridurongrit S, Lu MM, Epstein JA (2004) Cardiac outflow tract defects in mice lacking ALK2 in neural crest cells. Development 131:3481–3490
36. Kirby ML, urnage KL 3rd, Hays BM (1985) Characterization of conotruncal malformations following ablation of "cardiac" neural crest. Anat Rec 213:87–93
37. Li J, Molkentin JD, Colbert MC (2001) Retinoic acid inhibits cardiac neural crest migration by blocking c-Jun N-terminal kinase activation. Dev Biol 232:351–361
38. Nakamura T, Colbert MC, Robbins J (2006) Neural crest cells retain multipotential characteristics in the developing valves and label the cardiac conduction system. Circ Res 98:1547–1554
39. Stoller JZ, Epstein JA (2005) Cardiac neural crest. Semin Cell Dev Biol 16:704–715
40. St Amand TR, Lu JT, Chien KR (2003) Defects in cardiac conduction system lineages and malignant arrhythmias: developmental pathways and disease. Novartis Found Symp 250:260–270 (discussion 271–265, 276–269)
41. St Amand TR, Lu JT, Zamora M, Gu Y, Stricker J, Hoshijima M, Epstein JA, Ross JJ, Ruiz-Lozano P, Chien KR (2006) Distinct roles of HF-1b/Sp4 in ventricular and neural crest cells lineages affect cardiac conduction system development. Dev Biol 291:208–217
42. Van Kempen MJ, Vermeulen JL, Moorman AF, Gros D, Paul DL, Lamers WH (1996) Developmental changes of connexin40 and connexin43 mRNA distribution patterns in the rat heart. Cardiovasc Res 32:886–900
43. Waldo KL, Lo CW, Kirby ML (1999) Connexin 43 expression reflects neural crest patterns during cardiovascular development. Dev Biol 208:307–323
44. Xu X, Francis R, Wei CJ, Linask KL, Lo CW (2006) Connexin 43-mediated modulation of polarized cell movement and the directional migration of cardiac neural crest cells. Development 133:3629–3639
45. Liu S, Liu F, Schneider AE, St Amand T, Epstein JA, Gutstein DE (2006) Distinct cardiac malformations caused by absence of connexin 43 in the neural crest and in the non-crest neural tube. Development 133:2063–2073
46. Xu X, Li WE, Huang GY, Meyer R, Chen T, Luo Y, Thomas MP, Radice GL, Lo WW (2001) N-cadherin and Cx43alpha1 gap junctions modulates mouse neural crest cell motility via distinct pathways. Cell Commun Adhes 8:321–324
47. Li WE, Waldo K, Linask KL, Chen T, Wessels A, Parmacek MS, Kirby ML, Lo CW (2002) An essential role for connexin43 gap junctions in mouse coronary artery development. Development 129:2031–2042
48. Reaume AG, de Sousa PA, Kulkarni S, Langille BL, Zhu D, Davies TC, Juneja SC, Kidder GM, Rossant J (1995) Cardiac malformation in neonatal mice lacking connexin43. Science 267:1831–1834
49. Sullivan R, Huang GY, Meyer RA, Wessels A, Linask KK, Lo CW (1998) Heart malformations in transgenic mice exhibiting dominant negative inhibition of gap junctional communication in neural crest cells. Dev Biol 204:224–234
50. Choudhary B, Ito Y, Makita T, Sasaki T, Chai Y, Sucov HM (2006) Cardiovascular malformations with normal smooth muscle differentiation in neural crest-specific type II TGFbeta receptor (Tgfbr2) mutant mice. Dev Biol 289:420–429
51. Jiang X, Rowitch DH, Soriano P, McMahon AP, Sucov HM (2000) Fate of the mammalian cardiac neural crest. Development 127:1607–1616
52. Waller BR 3rd, McQuinn T, Phelps AL, Markwald RR, Lo CW, Thompson RP, Wessels A (2000) Conotruncal anomalies in the trisomy 16 mouse: an immunohistochemical analysis with emphasis on the involvement of the neural crest. Anat Rec 260:279–293

53. Aoyama N, Yamashina S, Poelmann RE, Gittenberger-De Groot AC, Izumi T, Soma K, Ohwada T (2002) Conduction system abnormalities in rat embryos induced by maternal hyperthermia. Anat Rec 267:213–219
54. Blom NA, Gittenberger-de Groot AC, DeRuiter MC, Poelmann RE, Mentink MM, Ottenkamp J (1999) Development of the cardiac conduction tissue in human embryos using HNK-1 antigen expression: possible relevance for understanding of abnormal atrial automaticity. Circulation 99:800–806
55. Chau MD, Tuft R, Fogarty K, Bao ZZ (2006) Notch signaling plays a key role in cardiac cell differentiation. Mech Dev 123:626–640
56. Erickson CA, Loring JF, Lester SM (1989) Migratory pathways of HNK-1-immunoreactive neural crest cells in the rat embryo. Dev Biol 134:112–118
57. Kise K, Nakagawa M, Okamoto N, Hanato T, Watanabe N, Nishijima S, Fujino H, Takeuchi Y, Shiraishi I (2005) Teratogenic effects of bis-diamine on the developing cardiac conduction system. Birth Defects Res A Clin Mol Teratol 73:547–554
58. Nagase T, Sanai Y, Nakamura S, Asato H, Harii K, Osumi N (2003) Roles of HNK-1 carbohydrate epitope and its synthetic glucuronyltransferase genes on migration of rat neural crest cells. J Anat 203:77–88
59. Nakagawa M, Thompson RP, Terracio L, Borg TK (1993) Developmental anatomy of HNK-1 immunoreactivity in the embryonic rat heart: co-distribution with early conduction tissue. Anat Embryol (Berl) 187:445–460
60. Nishida A, Kobayashi T, Ariyuki F (1997) In vitro developmental toxicity of concanavalin A in rat embryos: analysis of neural crest cell migration using monoclonal antibody HNK-1. Teratog Carcinog Mutagen 17:103–114
61. Wenink AC, Symersky P, Ikeda T, DeRuiter MC, Poelmann RE, Gittenberger-de Groot AC (2000) HNK-1 expression patterns in the embryonic rat heart distinguish between sinuatrial tissues and atrial myocardium. Anat Embryol (Berl) 201:39–50
62. Cantor AB, Orkin SH (2005) Coregulation of GATA factors by the Friend of GATA (FOG) family of multitype zinc finger proteins. Semin Cell Dev Biol 16:117–128
63. Molkentin JD (2000) The zinc finger-containing transcription factors GATA-4, -5, and -6. Ubiquitously expressed regulators of tissue-specific gene expression. J Biol Chem 275:38949–38952
64. Peterkin T, Gibson A, Loose M, Patient R (2005) The roles of GATA-4, -5 and -6 in vertebrate heart development. Semin Cell Dev Biol 16:83–94
65. Clegg MS, Keen CL, Lonnerdal B, Hurley LS (1981) Influence of ashing techniques in the analysis of trace elements in animal tissue. I. Wet ashing. Biol Trace Element Res 3:107–115
66. Hoffman JI, Kaplan S (2002) The incidence of congenital heart disease. J Am Coll Cardiol 39:1890–1900
67. Tanner K, Sabrine N, Wren C (2005) Cardiovascular malformations among preterm infants. Pediatrics 116:e833–838
68. Record IR, Tulsi RS, Dreosti IE, Fraser FJ (1985) Cellular necrosis in zinc-deficient rat embryos. Teratology 32:397–405
69. Chimienti F, Seve M, Richard S, Mathieu J, Favier A (2001) Role of cellular zinc in programmed cell death: temporal relationship between zinc depletion, activation of caspases, and cleavage of Sp family transcription factors. Biochem Pharmacol 62:51–62
70. Cartwright MM, Tessmer LL, Smith SM (1998) Ethanol-induced neural crest poptosis is coincident with their endogenous death, but is mechanistically distinct. Alcohol Clin Exp Res 22:142–149
71. Nishijima S, Nakagawa M, Fujino H, Hanato T, Okamoto N, Shimada M (2000) Teratogenic effects of bis-diamine on early embryonic rat heart: an in vitro study. Teratology 62:115–122
72. Boot MJ, Gittenberger-De Groot AC, Van Iperen L, Hierck BP, Poelmann RE (2003) Spatiotemporally separated cardiac neural crest subpopulations that target the outflow tract septum and pharyngeal arch arteries. Anat Rec A Discov Mol Cell Evol Biol 275:1009–1018
73. Baker CV, Bronner-Fraser M, Le Douarin NM, Teillet MA (1997) Early- and late-migrating cranial neural crest cell populations have equivalent developmental potential in vivo. Development 124:3077–3087
74. Kirby MK (2002) Molecular embryogenesis of the heart. Pediatr Dev Pathol 5:516–543
75. Echetebu CO, Ali M, Izban MG, MacKay L, Garfield RE (1999) Localization of regulatory protein binding sites in the proximal region of human myometrial connexin 43 gene. Mol Hum Reprod 5: 757–766
76. Teunissen BE, Jansen AT, van Amersfoorth SC, O'Brien TX, Jongsma HJ, Bierhuizen MF (2003) Analysis of the rat connexin 43 proximal promoter in neonatal cardiomyocytes. Gene 322:123–136
77. Meerarani P, Reiterer G, Toborek M, Hennig B (2003) Zinc modulates PPARgamma signaling and activation of porcine endothelial cell. J Nutr 133:3058–3064
78. Oteiza PI, Clegg MS, Zago MP, Keen CL (2000) Zinc deficiency induces oxidative stress and AP-1 activation in 3T3 cells. Free Radic Biol Med 28:1091–1099

79. Gonzalez-Reyes S, Fernandez-Dumont V, Calonge WM, Martinez L, Tovar JA (2006) Expression of Connexin 43 in the hearts of rat embryos exposed to nitrofen and effects of vitamin A on it. Pediatr Surg Int 22:61–65
80. Boot MJ, Gittenberger-de Groot AC, Poelmann RE, Gourdie RG (2006) Connexin43 levels are increased in mouse neural crest cells exposed to homocysteine. Birth Defects Res A Clin Mol Teratol 76:133–137
81. Huang GY, Cooper ES, Waldo K, Kirby ML, Gilula NB, Lo CW (1998) Gap junction-mediated cell-cell communication modulates mouse neural crest migration. J Cell Biol 143:1725–1734
82. Gutstein DE, Morley GE, Tamaddon H, Vaidya D, Schneider MD, Chen J, Chien KR, Stuhlmann H, Fishman GI (2001) Conduction slowing and sudden arrhythmic death in mice with cardiac-restricted inactivation of connexin43. Circ Res 88:333–339
83. Lo CW, Cohen MF, Huang GY, Lazatin BO, Patel N, Sullivan R, Pauken C, Park SM (1997) Cx43 gap junction gene expression and gap junctional communication in mouse neural crest cells. Dev Genet 20:119–132